Patel, D. J., Kozlowski, S. A., Ikuta, S., Itakura, K., Bhatt, R., & Hare, D. H. (1982) *Cold Spring Harbor Symp. Quant. Biol. 47*, 197–206.
Rinkel, L. J., & Altona, C. (1987) *J. Biomol. Struct. Dyn. 4*, 621–649.
Scheek, R. M., Russo, N., Boelens, R., Kaptein, R., & Van Boom, J. H. (1983) *J. Am. Chem. Soc. 105*, 2914–2916.
Scheek, R. M., Boelens, R., Russo, N., van Boom, J. H., & Kaptein, R. (1984) *Biochemistry 23*, 1371–1376.
Senior, M., Jones, R. A., & Breslauer, K. J. (1988) *Biochemistry 27*, 3879–3885.
Sklenar, V., & Bax, A. (1987) *J. Am. Chem. Soc. 109*, 7525–7526.
Sklenar, V., Miyashiro, H., Zon, G., Miles, T. A., & Bax, A. (1986) *FEBS Lett. 208*, 94–98.
Uesugi, S., Shida, T., & Ikehara, M. (1981) *Chem. Pharm. Bull. 29*, 3573–3585.
Usman, N., Ogilvie, K. K., Jiang, M. Y., & Cedergven, R. J. (1987) *J. Am. Chem. Soc. 109*, 7845–7854.
Weiner, P. K., & Kollman, P. A. (1981) *J. Comput. Chem. 2*, 287–303.
Wemmer, D. E., Chou, S., Hare, D. R., & Reid, B. R. (1985) *Nucleic Acids Res. 13*, 3755–3772.
Wilbur, D. W., DeFries, T., & Jonas, J. (1976) *J. Chem. Phys. 65*, 1783.
Williamson, J. R. (1988) Ph.D. Thesis, Stanford University.
Williamson, J. R., & Boxer, S. G. (1988) *Nucleic Acids Res. 16*, 1529–1540.
Wüthrich, K. (1986) *NMR of Proteins and Nucleic Acids*, Wiley, New York.

Multinuclear NMR Studies of DNA Hairpins. 2. Sequence-Dependent Structural Variations†

James R. Williamson‡ and Steven G. Boxer*
Department of Chemistry, Stanford University, Stanford, California 94305
Received September 8, 1988; Revised Manuscript Received December 8, 1988

ABSTRACT: The solution conformation of three related DNA hairpins, each with five bases in the loop, is investigated by proton and phosphorus 2D NMR methods. The sequences of the three oligomers are d(CGCGTTGTTCGCG), d(CGCGTTTGTCGCG), and d(CTGCTCTTGTTGAGCAG). One pair of hairpins shares the same stem sequence but differs in the loop, and the appearance of an unusual phosphate torsion in the stem is found to depend on the sequence in the loop of the hairpin. The second pair of hairpins shares the same loop region but differs in the stem sequence in that the base pair which closes the loop is a C-G or G-C pair. The pattern of NOEs reveals that the stacking arrangement in the loop region depends on the base pair that closes the stem. These results suggest that hairpin loop conformation and dynamics are sensitive to small changes in the loop and adjacent stem sequences. These findings are discussed in relation to sequence-dependent thermodynamic changes that have been observed in RNA hairpins.

In the preceding paper, the solution structure of the DNA hairpin formed by d(CGCGTTGTTCGCG) was studied in detail. Some unusual features in this structure were revealed by multinuclear NMR studies in the region of the junction between the stem and the loop regions. A phosphorus resonance, assigned to P_{10}, was shifted downfield, and this was interpreted as a phosphate in the t,g$^-$ conformation. This phosphate, located one base away from the junction of the stem and loop, exhibits relatively slow exchange between two or more conformations at intermediate temperatures. This is accompanied by upfield shifts of the nearby base protons in the loop region. The stacking of the two loop bases T_8 and T_9 over the stem changed slightly in a premelting transition. The other three bases in the loop of this hairpin were also found to stack over the other side of the stem region.

To investigate the possibility of a sequence effect on hairpin conformation, two new sequences were designed and synthesized. For purposes of discussion, the three hairpin sequences will be referred to as follows:

hairpin I

d(CGCG-TTGTT-CGCG)

hairpin II

d(CGCG-TTTGT-CGCG)

hairpin III

d(CTGCTC-TTGTT-GAGCAG)

Hairpin I is the subject of a detailed structural investigation (Williamson & Boxer, 1989). Hairpin II is identical with hairpin I except that the G in the loop has been shifted one position toward the 3′ end of the sequence. This sequence was designed to examine the effect of loop sequence on the conformation of the hairpin. Hairpin III was designed to test the effect of the stem sequences on the loop conformation. The sequence in the loop (TTGTT) is the same as that of hairpin I, but the important difference is that the loop in hairpin III is closed by a G-C pair, while the loop in hairpin I is closed by a C-G pair. All of the sequence share the common feature of a loop region consisting of five bases.

Hairpins II and III were not characterized in as great detail as hairpin I (see preceding paper). Proton and phosphorus NMR spectra were partially assigned by using 2D methods. NOEs[1] were not quantitated to obtain distances, but rather

† This work was supported by a grant from the National Institutes of Health (R01 GM27738). S.G.B. is the recipient of a Presidential Young Investigator Award.
‡ Present address: Department of Chemistry and Biochemistry, University of Colorado, Boulder, CO 80309.

0006-2960/89/0428-2831$01.50/0

a qualitative analysis of the pattern and magnitude of the NOEs was performed. By simple comparison with the data for hairpin I whose structure is known in detail, the similarities and differences in the structure of related sequences can quickly be assessed.

Materials and Methods

The DNA molecules d(CGCGTTTGTCGCG) and d(CTGCTCTTGTTGAGCAG) were synthesized by phosphoramidite chemistry and were purified by reverse-phase HPLC. Samples were desalted on a low-pressure reverse-phase column, the desired buffers were added, and the solvent was exchanged for D_2O by repeated concentration from 99.8% D_2O on a Speed-Vac. Sample conditions were 70 mM NaCl, 35 mM sodium phosphate, pH 7.0 (meter reading), and 5 mM EDTA, and all spectra presented in the figures were recorded at 25 °C. The oligonucleotide concentration was ~1.5 mM for hairpin II and ~3 mM for hairpin III.

NMR Measurement. Proton spectra were recorded at 500 MHz and phosphorus spectra were recorded at 202 MHz on a GE GN-500 spectrometer. Proton chemical shifts are referenced to (trimethylsilyl)propionic-d_4 acid internal standard, and phosphorus shifts are referenced to trimethyl phosphate external standard. Proton–phosphorus correlation was performed by using a proton-detected version of the standard heteronuclear correlation experiment (Sklenar et al., 1986).

Results

In the previous paper hairpin I was shown unambiguously to adopt a hairpin conformation on the basis of a variety of data. The melting behavior was independent of concentration, and relaxation measurement indicated that the rotational correlation time was consistent with the dimensions of the hairpin structure. No extensive experimentation was done to demonstrate the hairpin conformation for hairpins II and III. However, there is some credible evidence to support the assertion that they also adopt a hairpin conformation. The melting temperatures for hairpins II and III are both in excess of 70 °C. Unpaired imino protons are observable in the 10–11 ppm region that are characteritic of loop regions. Also there is a break in the NOE connectivity in the loop regions that appears to be characteristic of loop structure in hairpins (vide infra). In addition, only one set of resonances was observed in the proton and phosphorus spectra at all temperatures for both molecules.

Proton NMR Data

Studies of the Hairpin d(CGCGTTTGTCGCG). The proton NMR spectrum of hairpin II is very similar to that of hairpin I. The H1′, H2′, H2″, H3′, and base protons for hairpin II were completely assigned from a NOESY spectrum. An expansion of the base proton to H1′ cross-peak region of the NOESY spectrum is shown in Figure 1a, and an expansion of the base proton to H2′/H2″ region is shown in Figure 1b. The assignments were obtained by using the sequential assignment procedure, and as found for hairpin I in the preceding paper, there is a break in the sequential assignment pathway midway through the sequence. The pattern of NOEs can be followed from the 5′ end through to residue T_7, where there is a break. The sequential assignment pathway resumes at residue C_{10} and continues to the 3′ end of the sequence. The pattern of NOEs in the base proton to H2′/H2″ region is similar to that in the base proton to H1′ region, with additional contacts between protons on residues G_8 and T_9, and T_9 and C_{10}. A listing of the assignments is presented in Table I.

The stem region of hairpin II appears to consist of four C-G base pairs in a B-DNA conformation as evidenced by the pattern and magnitude of the NOEs in that region. The pattern of cross peaks in the NOESY spectrum in the stem region is nearly superimposable on the same region in the NOESY spectrum of hairpin I. This is strong evidence for similar structure in the stem region of the two hairpins.

The pattern of NOEs in the loop region is also very similar to that of hairpin I, in that there is a break in the NOE connectivity between the third and fourth positions in the loop. Stacking interactions are present in the loop region and between the stem and the loop as evidenced by the B-DNA-like pattern of NOEs in that region.

Hairpin III: d(CTGCTCTTGTTGAGCAG). The appearance of the proton NMR spectrum of hairpin III is quite different from that of the other two due to the completely

Table I: Chemical Shift Assignments for Hairpin II, d(CGCGTTTGTCGCG), at 25 °C[a]

residue	H6/H8	H1′	$H2_d$[b]	$H2_u$[b]	H3′	H5/CH_3	^{31}P
C_1	7.67	5.79	2.44	2.00	4.73	5.94	−3.76
G_2	8.00	5.94	2.77	2.72	5.00		−3.87[c]
C_3	7.34	5.80	2.34	1.89	4.85	5.48	ND[d]
G_4	7.86	6.07	2.67	2.59	4.98		−3.65
T_5	7.41	6.04	2.45	2.23	4.87	1.77	−3.70
T_6	7.58	6.05	2.39	2.11	4.67	1.83	−4.23
T_7	7.43	5.91	2.15	1.90	4.61	1.69	−3.89
G_8	7.82	6.09	2.88	2.68	4.95		ND[d]
T_9	7.56	6.21	2.52	2.31	4.82	1.84	−3.52[e]
C_{10}	7.53	5.53	2.38	1.96	4.81	5.78	−3.72[e]
G_{11}	7.98	5.93	2.74	2.70	5.01		−3.87[c]
C_{12}	7.38	5.84	2.37	1.93	4.85	5.51	ND[d]
G_{13}	7.97	6.19	2.72	2.63	4.70		

[a] Proton shifts are reported in ppm downfield from TSP internal standard and phosphorus shifts in ppm downfield from trimethyl phosphate external standard. [b] H2′ and H2″ were not unambiguously differentiated, but in general $H2_u$ = H2′ and $H2_d$ = H2″. [c] H3′ and phosphate resonances are coincident. [d] ND = assignment could not be determined. [e] H3′ resonances are coincident; therefore, phosphate assignment is ambiguous between residues T_9 and C_{10}.

Table II: Chemical Shift Assignments for Hairpin III, d(CTGCTCTTGTTGAGCAG), at 25 °C[a]

residue	H6/H8	H1′	$H2_u$[b]	$H2_d$[b]	H3′	H5/CH_3/ H2	^{31}P
C_1	7.85	5.95	2.59	2.17	4.71	5.96	−3.91[c]
T_2	7.52	5.86	2.57	2.24	4.93	1.73	−3.78
G_3	7.98	5.96	2.76	2.76	5.04		−3.65
C_4	7.50	5.99	2.58	2.17	4.73	5.40	−4.12[d]
T_5	7.51	6.11	2.54	2.17	4.90	1.68	−3.93
C_6	7.62	6.15	2.46	2.27	4.86	5.72	−3.82
T_7	7.46	6.10	2.44	2.22	4.84	1.79	−3.64
T_8	7.45	6.03	2.28	1.97	4.69	1.82	−3.91[c]
G_9	7.87	5.99	2.62	2.51	4.69		−3.91[c]
T_{10}	7.46	6.08	2.41	2.24	4.77	1.66	−3.92
T_{11}	7.40	5.82	2.32	1.97	4.74	1.83	−4.12[d]
G_{12}	8.00	5.42	2.79	2.71	4.99		−3.62
A_{13}	8.20	6.14	2.94	2.76	5.10	7.83	−3.89
G_{14}	7.70	5.80	2.67	2.52	5.00		−3.79
C_{15}	7.34	5.55	2.29	1.91	4.82	5.35	−3.91
A_{16}	8.22	6.08	2.90	2.73	5.05	7.85	−3.80
G_{17}	7.75	6.07	2.48	2.32	4.67		

[a] Proton shifts are reported in ppm downfield from TSP internal standard and phosphorus shifts in ppm downfield from trimethyl phosphate external standard. [b] H2′ and H2″ were not unambiguously differentiated, but in general $H2_u$ = H2′ and $H2_d$ = H2″. [c] H3′ and phosphate resonances are coincident. [d] H3′ and phosphate resonances are coincident.

[1] Abbreviations: NOE, nuclear Overhauser effect; HPLC, high-performance liquid chromatography; EDTA, ethylenediaminetetraacetic acid; ppm, parts per million; NOESY, nuclear Overhauser effect spectroscopy.

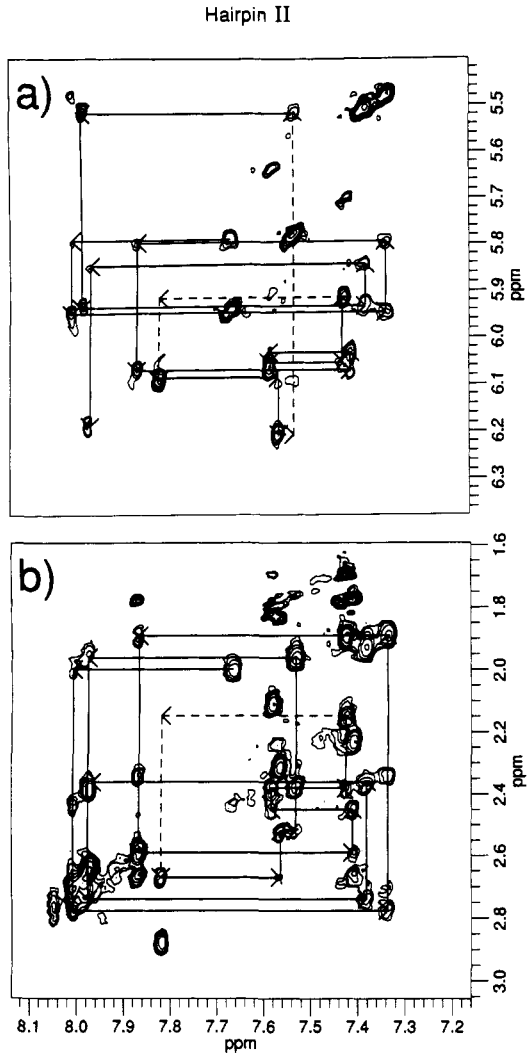

FIGURE 1: NOESY spectrum of d(CGCGTTTGTCGCG), hairpin II. A total of 64 accumulations of 1024-point real and imaginary spectra were recorded for 238 t_1 values with a mixing time of 400 ms. (a) Expansion of the region containing the cross peaks between the base protons and the H1′ protons. The sequential assignment pathway is shown with arrows: solid arrows denote contacts that are observed, and dotted arrows indicate where the expected cross peak is missing. (b) Expansion of the cross-peak region between the base protons and the H2′/H2″ protons, with the sequential assignment pathway denoted by arrows. Cross peaks at 5.62 and 5.70 ppm are due to strong NOEs from a minor decomposition product.

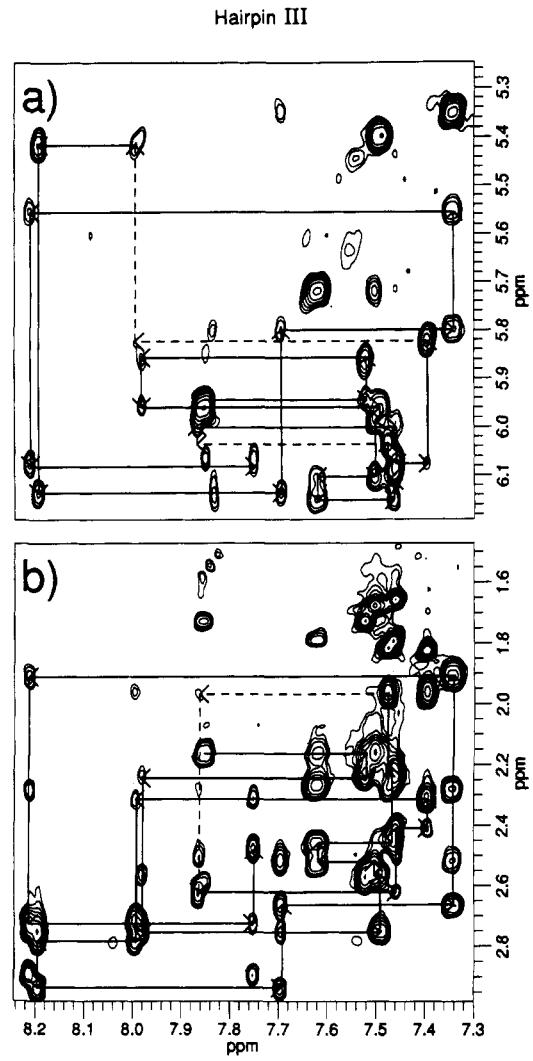

FIGURE 2: NOESY spectrum of d(CTGCTCTTGTTGAGCAG), hairpin III. A total of 32 accumulations of 1024-point real and imaginary spectra were recorded for 512 t_1 values with a mixing time of 350 ms. (a) Expansion of the region containing the cross peaks between the base protons and the H1′ protons. The sequential assignment pathway is shown with arrows: solid arrows denote contacts that are observed, and dotted arrows indicate where the expected cross peak is missing. (b) Expansion of the cross-peak region between the base protons and the H2′/H2″ protons, with the sequential assignment pathway denoted by arrows.

different sequence in the stem region. The proton resonances were assigned from a NOESY spectrum, and the assignments are listed in Table II. An expansion of the base to H1′ cross peaks for hairpin III is shown in Figure 2a with the sequential assignment pathway. Two breaks are observed in this pathway, one between residues T_8 and G_9 and one between residues T_{11} and G_{12}. The sequential pathway for the base to H2′ contacts is shown in Figure 2b. The only break in this pathway is between residues T_8 and G_9. The stem region of hairpin III also appears to exist in the typical B-DNA conformation. As with the two other hairpins, the pattern of NOEs indicates that there is stacking of the loop bases over the stem and with each other.

Phosphorus NMR Data

The phosphorus NMR spectrum for hairpin II is shown in Figure 3b, and the spectrum of hairpin I is shown for comparison in Figure 3c. Unlike hairpin I, there is no downfield-shifted phosphate in hairpin II, but rather one phosphate is shifted upfield. The phosphorus spectrum of hairpin III is shown in Figure 3a, and it exhibits no upfield- or downfield-shifted resonances. The differences in the phosphorus spectra reflect significant differences in the backbone torsions in the three hairpins.

The phosphorus resonances in hairpin II were partially assigned with a phosphorus–proton correlation experiment that is shown in Figure 4. The phosphate phosphorus is scalar-coupled to the H3′ proton of the preceding residue, as well as to the H4′ and H5′/H5″ protons on the next residue. The phosphate assignments were made on the basis of the coupling to the H3′ protons, which were completely assigned from the NOESY spectra. The upfield-shifted phosphate in hairpin II is clearly assigned to P_6, which is between residues T_6 and T_7. The resonance for P_{10}, which is downfield shifted in hairpin I, is not shifted in hairpin II and appears at the normal chemical shift for a B-DNA phosphate. The chemical shifts of the other phosphorus resonances that were assigned are also listed in Table I.

The phosphorus resonances in hairpin III were also partially assigned by a heteronuclear correlation experiment, and a plot

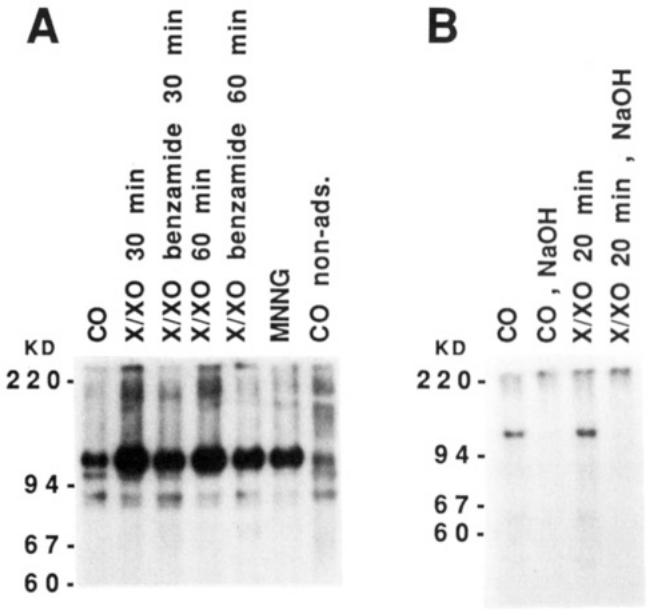

FIGURE 2: ADPR-transferase immunoblots of acid-insoluble nuclear material from JB6 (clone 41) cells that had been treated with active oxygen or *N*-methyl-*N'*-nitro-*N*-nitrosoguanidine. Experimental conditions were as described in the legend to Figure 1 and under Methods. A polyclonal rabbit anti-ADPR-transferase antibody was used and reacted with ^{125}I-labeled donkey anti-rabbit Ig for autofluorography. (A) Induction of poly(ADP-ribosylation) by active oxygen and MNNG, respectively, and effect of the ADPR-transferase inhibitor benzamide (100 μM). (B) Removal of poly(ADPR) chains from ADPR-transferase by treatment of nuclear preparations with 0.1 N NaOH as described under Methods.

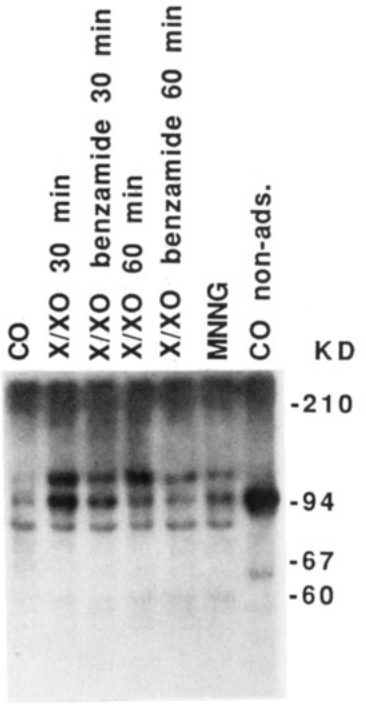

FIGURE 3: Topoisomerase I immunoblots of acid-insoluble nuclear material from JB6 (clone 41) cells that had been treated with active oxygen or *N*-methyl-*N'*-nitro-*N*-nitrosoguanidine. Experimental conditions were as described in the legend to Figure 1 and under Methods. A polyclonal rabbit anti-topoisomerase I antibody was used and reacted with ^{125}I-labeled donkey anti-rabbit Ig for autofluorography.

for the 95-kDa band were directly proportional to the amounts of [^{3}H]leucine protein radioactivity applied on the gel (see Figure 1B), allowing the calculation of the extent of poly-

Table II: Poly(ADP-ribosylation) of Topoisomerase I by Active Oxygen (JB6 Clone 41)

	normalized densitometer readings[b]	poly(ADP-ribosylation) of topoisomerase I (%)
adsorbed on boronate[a]		
control	4.2	0.11
X/XO, 30 min	25.5	0.68
X/XO + benzamide, 30 min	10.8	0.29
X/XO, 60 min	5.0	0.13
X/XO + benzamide, 60 min	3.6	0.10
MNNG, 20 min	9.3	0.25
nonadsorbed on boronate control	3704	

[a] Cells exposed to active oxygen (X/XO 50/5 μg/mL), active oxygen plus benzamide (100 μM), or MNNG (5 μg/mL) for the indicated lengths of time. [b] Densitometer readings of the 95-kDa band from Western blots normalized to 1% of the total nuclear proteins from 1.4 $\times$ 10^8 cells.

(ADPR) substitution of topoisomerase I. From the data listed in Table II, it is evident that the extent of steady-state substitution of topoisomerase I with poly(ADPR) is low (0.11%), that AO treatment caused a 6-fold increase within 30 min, and that the level of substitution has essentially returned to control levels within 60 min.

Discussion

In general, it has not been possible to selectively radioactively label the cellular NAD pool with ^{32}P in intact cells. While labeling of NAD with [^{3}H]adenosine (Aldolph & Song, 1985a,b) or [^{3}H]adenine (Cardenas-Corona et al., 1987) has been successful, the radioactivity associated with many poly(ADPR) acceptor proteins is insufficient for fluorometry. This represents a major obstacle for studies of the poly(ADP-ribosylation) of nuclear proteins in vivo. The experimental strategy combining phenylboronate PBA-30 affinity chromatography with immunoblots taken in the present work circumvents this difficulty. Since phenylboronate retains mono- and poly(ADP-ribosylated) proteins, our data do not yield information about the chain lengths of the substituents. However, since nuclear proteins were isolated mono(ADP-ribosylated) proteins probably result from the degradation of poly(ADPR) chains rather than bona fide ADP-ribosylation (Althaus & Richter, 1987; Althaus et al., 1985). The combination with immunoblots is necessary because of the limited specificity of the phenylboronate PBA-30 column. From our results with the antibody against poly(ADPR) chains (Figure 1), it is evident that PBA-30 effectively removed poly(ADP-ribosylated) proteins because no bands were visible in the nonadsorbed flow-through. However, PBA-30 in addition also retained non-poly(ADP-ribosylated) proteins. This is evident from the observation that the fraction of proteins retained always represented 1.3–1.5% of the total and did not increase upon treatment with inducers of poly(ADPR) synthesis. Therefore, retention on PBA-30 does not suffice for the identification of poly(ADPR) acceptor proteins. We used the following additional criteria: (1) detection by poly(ADPR) antibodies on immunoblots; (2) alkaline hydrolysis of the poly(ADPR) substituents; (3) increase in specific bands on immunoblots with antibodies against specific acceptor proteins; (4) inhibition of the reaction by the ADPR-transferase inhibitor benzamide. To avoid undesirable side reactions, low benzamide concentrations (100 μM) were used. Even under these conditions poly(ADP-ribosylation) was inhibited by more than 50%.

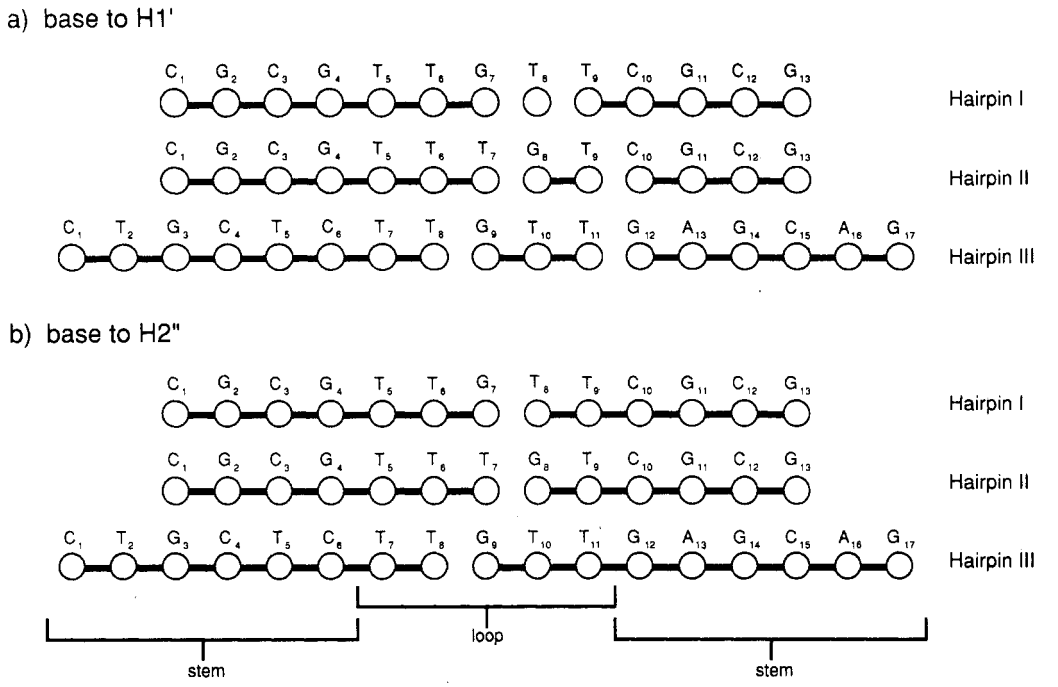

FIGURE 7: NOE connectivity patterns compared for three DNA hairpins: (a) base to H1′ proton pathway; (b) base to H2″ pathway.

for hairpins I and II show unusual upfield- or downfield-shifted resonances. The downfield-shifted phosphate in hairpin I was assigned to P_{10}, which is a phosphate group in the stem region of that molecule. The upfield-shifted phosphate in hairpin II was assigned to P_6, which is a phosphate in the loop region. Even though the stacking patterns in hairpins I and II appear to be similar, the unusual geometry around P_{10} found in hairpin I is apparently not present in hairpin II.

The differences in the structure of the three hairpins suggest that there is a complex interplay of stacking interactions that determines the structure of the loop regions. Hairpin I exhibits intermediate exchange between two conformations, which is apparent in the phosphorus spectrum at intermediate temperatures (Williamson & Boxer, 1989). The site of this conformational transition is near the junction between the 3′ portion of the stem and the loop region. The stacking arrangement in hairpin II is very similar to that in hairpin I, but there is no evidence for a conformational transition or unusual geometry at the stem–loop junction, as is seen in hairpin I. In hairpin I, there are upfield shifts of the base protons of residues T_8 and T_9 in the same temperature range as a conformational change in P_{10} from t,g to g,g$^-$. These data suggest that there are two slightly different stacking arrangements among the bases T_8, T_9, C_{10}, and G_{11} that are energetically close. In hairpin II, residue T_8 has been substituted by residue G_8, and in this case, there is no unusual phosphate conformation for P_{10}. By changing a single base, two residues removed, the backbone conformation is affected, presumably by the changes in the stacking interactions in the loop.

The stacking preferences for DNA and RNA hairpins have been rationalized in terms of interstrand phosphate distances in B-DNA and A-RNA (Haasnoot et al., 1986). For DNA hairpins, the stacking is predicted on the basis of these steric arguments to be three bases in the 5′ side of the loop and two bases in the 3′ side of the loop. While this is the arrangement we observe in hairpins I and II, a different arrangement is observed in hairpin III. Although the rationale for predicting loop stacking from steric constraints is reasonable and seems to apply in many cases, it is clear that the sequence of the loop and adjacent stem bases can also play a role in determining the loop conformation.

Extra stacked bases on a helix are more stable when stacked over the 3′ end of the helix for RNA (Sugimoto et al., 1987), while they are more stable stacked over the 5′ end of the helix for DNA (Senior et al., 1988), making it impossible to directly compare DNA and RNA hairpins. However, it is reasonable to expect that structural variations we observe in DNA hairpins may relate to the sequence-dependent stability that has been observed in RNA hairpins.

Sequence-dependent changes in the thermodynamic stability of RNA hairpins have been observed in several examples. One prevalent RNA hairpin sequence is the loop sequence UUCG closed by a C-G base pair that has been found in a wide variety of contexts (Tuerk et al., 1988). Single base changes in the loop region and reversing the closing base pair to a G-C reduce the stability of the hairpin. A common loop sequence found in many ribosomal RNAs (Woese et al., 1983), as well as the self-splicing RNA from *Tetrahymena thermophila*, is GAAA. Single base changes in the loop of GAAA hairpins also results in changes in thermodynamic stability, as does flipping the base pair that closes the loop from G-C to C-G (J. Haney and O. Uhlenbeck, unpublished results). A similar effect has been seen with the hairpin in the 3′ terminal colicin fragment of 16S RNA. Comparison of hairpins from different species revealed a change in T_m of 10 °C on changing the base pair closing the loop from C-G to G-C (Heus, 1987).

There are at least three competing factors that appear to influence hairpin loop conformation. The first is the steric constraint for loop closure, which has been discussed in terms of interstrand phosphate distances (Haasnoot et al., 1986). The second factor is the stacking energy of the loop bases over the stem bases, for which some thermodynamic data exist (Senior et al., 1988; Sugimoto et al., 1987). The third factor is the stacking energy of the loop bases among themselves, for which no thermodynamic data yet exist. The steric factor and the helix–loop stacking are opposing forces in both DNA and RNA in that the arrangement which is thermodynamically favored is the opposite to the arrangement which is sterically favored. In hairpins I and II, the steric factor apparently prevails, while in hairpin III, the stem–loop stacking prevails. The effects of stacking among the loop bases are perhaps more subtle, but the backbone conformations at P_{10} in hairpins I

and II are definitely different, possibly due to slight changes in the stacking of the loop bases.

These studies on a set of related sequences indicate that there can be a substantial effect of the nucleotide sequence on the conformational properties of DNA hairpins. Most of the DNA hairpins studied to date have loop regions that consist solely of thymidine residues (Haasnoot et al., 1980, 1983; Hare & Reid, 1986; Ikuta et al., 1986). By studying a diverse set of sequences, both RNA and DNA, with different combinations of stem sequences, loop sequences, and loop sizes, we can approach a comprehensive understanding of hairpin structure. We are currently undertaking a study of the thermodynamics of this set of related hairpins to look for a correlation of the structural variations with stability.

ACKNOWLEDGMENTS

The 500-MHz NMR spectrometer was funded by grants from the National Science Foundation (DMB-8515942) and from the National Institutes of Health (1-51-RR-2733-01). We thank Dr. Jack Ohlms and Karen Wert at Beckman Instruments, Palo Alto, CA, for the generous gift of d(CTGCTCTTGTTGAGCAG). We also thank Dr. Hans Heus for helpful comments on the manuscript.

Registry No. Hairpin I, 115427-43-5; hairpin II, 119242-88-5; hairpin III, 119242-93-2.

REFERENCES

Giessner-Prettre, C., Pullman, B., Prado, F. R., Cheng, D. M., Iuorno, V., & Ts'o, P. O. P. (1984) *Biopolymers 23*, 377-388.

Gorenstein, D. G., & Luxon, B. A. (1979) *Biochemistry 18*, 3796-3804.

Haasnoot, C. A. G., den Hartog, J. H. J., de Rooij, J. F. M., van Boom, J. H., & Altona, C. (1980) *Nucleic Acids Res. 8*, 169-181.

Haasnoot, C. A. G., de Bruin, S. H., Berendsen, R. G., Janssen, H. G. J. M., Binnendijk, T. J. J., & Hilbers, C. W. (1983) *J. Biomol. Struct. Dyn. 1*, 115-128.

Haasnoot, C. A. G., Hilbers, C. W., van der Marel, G. A., van Boom, J. H., Singh, U. C., Pattabiraman, N., & Kollman, P. A. (1986) *J. Biomol. Struct. Dyn. 3*, 843-857.

Hare, D. R., & Reid, B. R. (1986) *Biochemistry 25*, 5341-5350.

Heus, H. A. (1987) Ph.D. Thesis, State University of Leiden, The Netherlands.

Ikuta, S., Chattopadhyaya, R., Ito, H., Dickerson, R. E., & Kearns, D. R. (1986) *Biochemistry 25*, 4840-4849.

Senior, M., Jones, R. A., & Breslauer, K. J. (1988) *Biochemistry 27*, 3879-3885.

Sklenar, V., Miyashiro, H., Zon, G., Miles, T. A., & Bax, A. (1986) *FEBS Lett. 208*, 94-98.

Sugimoto, N., Kierzek, R., & Turner, D. H. (1987) *Biochemistry 26*, 4554-4558.

Tuerk, C., Gauss, P., Thermes, C., Groebe, D. R., Gayle, M., Guild, N., Stormo, G., D'Aubenton-Carafa, Y., Uhlenbeck, O. C., Tinoco, I., Jr., Brody, E. N., & Gold, L. (1988) *Proc. Natl. Acad. Sci. U.S.A. 85*, 1364-1368.

Williamson, J. R., & Boxer, S. G. (1989) *Biochemistry* (preceding paper in this issue).

Woese, C. R., Gutell, R., Gupta, R., & Noller, H. F. (1983) *Microbiol. Rev. 47*, 621-669.

Mutation Induced in Vitro on a C-8 Guanine Aminofluorene Containing Template by a Modified T7 DNA Polymerase†

Janet Sahm, Edith Turkington, Diane LaPointe, and Bernard Strauss*

Department of Molecular Genetics and Cell Biology, The University of Chicago, Chicago, Illinois 60637

Received August 9, 1988; Revised Manuscript Received November 18, 1988

ABSTRACT: We reacted uracil-containing M13mp2 DNA with *N*-hydroxy-2-aminofluorene to produce a template with *N*-(deoxyguanosin-8-yl)-2-aminofluorene adducts. This template was hybridized to a non-uracil-containing linear fragment from which the *lac z* complementing insert had been removed to produce a gapped substrate. DNA synthesis using this substrate with the modified T7 DNA polymerase Sequenase led to an increase in the number and frequency of *lac*$^-$ mutations observed. *Escherichia coli* DNA polymerase I (Kf) did not yield a comparable increase in mutation frequency or number even though both Sequenase and the *E. coli* polymerase had similar, low, 3′ → 5′ exonuclease activities as compared to T4 DNA polymerase. We did not observe an increase in mutations when synthesis was attempted on a template reacted with *N*-acetoxy-2-(acetylamino)fluorene to give *N*-(deoxyguanosin-8-yl)-2-(acetylamino)fluorene adducts. Both *E. coli* and T7 enzymes terminate synthesis before all (acetylamino)fluorene lesions. Only some of the putative aminofluorene adducts produced strong termination bands, and there was a difference in the pattern generated by Sequenase and *E. coli* pol I (Kf) using the same substrate. Analysis of the mutations obtained from Sequenase synthesis on the aminofluorene-containing templates indicated a preponderance of −1 deletions at G's and of G → T transversions.

Most mutations occur as a result of errors during replication. A large literature deals with the problem of the fidelity of polymerases synthesizing DNA on normal templates (Kirkwood et al., 1986). An early analysis of the factors involved in mutation induced by prokaryotic polymerases which carry their own 3′ → 5′ exonucleases (Fersht, 1979) pointed out that the probability of fixing a mismatch depended on at least three factors: (a) the rate of incorporation of the mismatched base; (b) the rate of excision of the mismatch by the

† This work was supported in part by grants from the National Institute of General Medical Sciences (GM 07816) and the National Cancer Institute (CA32436) and by a contract with the Department of Energy (DE-AC02-76ER02040).

* Author to whom correspondence should be addressed.

0006-2960/89/0428-2836$01.50/0